Journal of Advanced Research in Applied Sciences and Engineering Technology

Journal homepage:
https://semarakilmu.com.my/journals/index.php/applied_sciences_eng_tech/index
ISSN: 2462-1943

Optical Simulation Study for Non-Invasive Jaundice Application: Effect of Bilirubin, Melanosome, LED Radial Width Distribution and Optode Distance

Nur Safwah Abd Rahaman[1], Nur Anida Jumadi[1,2,*], Audrey Huong Kah Ching[1,2], Wan Mahani Hafizah Wan Mahmud[1,2], Junaid Ali[3]

[1] Department of Electronic Engineering, Faculty of Electrical and Electronic Engineering, Universiti Tun Hussein Onn Malaysia, Parit Raja, 86400 Batu Pahat, Johor, Malaysia
[2] Principle Researcher in Advanced Medical Imaging and Optics (AdMedic), Universiti Tun Hussein Onn Malaysia, Parit Raja, 86400 Batu Pahat, Johor, Malaysia
[3] Optoelectronics Research Laboratory, COMSATS University Islamabad, Islamabad Capital Territory 45550, Pakistan

ABSTRACT

One of the promising diagnosis devices is the non-invasive bilirubin detection for estimating newborn jaundice. From the light interaction through tissue perspective, less attention has been given to the effect of LED radial width distribution at different melanosome content and bilirubin concentrations. Besides, different optode (emitter-detector) spacing can affect the light measured at the detector. This paper aims to investigate the effects of three LED radial width distributions (30°, 40° and 60°) on three types of skin pigmentation (light-skinned Caucasians, well-tanned Caucasians and Mediterranean, and dark-skinned pigmented Africans) based on hyperbilirubinemia and excessive hyperbilirubinemia conditions by using MCmatlab to simulate a 3D cuboid shape of neonatal forehead tissue layers. To mimic the tissues model, optical properties such as absorption coefficient (μ_a), reduced scattering coefficient ($'\mu_s$), and scattering anisotropy (g) were applied in every layer. Wavelength 470 nm was chosen since it is the most responsive wavelength at bilirubin's absorption spectra. Two optode spacing (0.7 cm and 2 cm) were used to demonstrate the effect of LED radial width. Main findings revealed that for all three types of skin, 30° LED radial width distribution resulted different trends in 0.7 cm and 2 cm of optode spacing. At 0.7 cm, a higher percentage of incident light was collected at the detector, whereas diffuse reflectance was lower. However, at a 2cm distance, both diffuse reflectance and the percentage of incident light collected on the detector were lower. These measured outcomes in diffuse reflectance on light skin were increased by six times, and the incident light collected was one time larger than on tanned and dark skin, as light skin colour absorbs less light and therefore gives a better reflection. Different optode spacing will be investigated for future studies as this information can serve as valuable input when designing optical hardware for non-invasive jaundice detection.

Keywords:
Optical simulation; Monte Carlo; Bilirubin; Melanosome; Matlab; Light propagation; LED radial width; On-invasive jaundice application

[*] *Corresponding author.*
E-mail address: anida@uthm.edu.my

https://doi.org/10.37934/araset.55.1.177190

1. Introduction

Non-invasive procedures restrict the number and amount of incisions made into the body or tissue removal, lowering the patient's risk of significant complications. As an example, without taking any blood sample, the pulse oximeter can estimate the amount of oxygen in the blood by using a light beam penetrating through the fingertip [1]. The same non-invasive technique is also introduced in bilirubin detection, as an alternative way to estimate serum bilirubin in blood without performing any blood test.

Bilirubin is an orange-yellow pigment produced by the breakdown of red blood cells [2]. It is essential to test bilirubin detection as the results can determine the newborn jaundice. The symptoms usually appear when the eyes and skin start turning yellow [3,4]. Increased bilirubin levels could be a sign of liver or bile duct issues. On rare occasions, increased haemolysis (the breakdown of red blood cells) can raise bilirubin levels and lead to liver complications or injury. Consequently, it is crucial to check for bilirubin levels, especially in neonates. If they have a high concentration of red blood cells, which are broken down often, they are more prone to jaundice. Because their liver is still developing, it is less efficient at excreting bilirubin and expelling it from the blood [5]. Several factors can affect the variability of bilirubin readings, including skin thickness, volume and blood flow, neonate maturity and skin pigmentation [7]. Besides, skin colour pigmentation also been widely considered by previous researchers in evaluating the diffuse reflectance spectrum of a jaundice neonate [6].

In general, melanocytes help determine skin, hair, and eye colours, and they are found in varying numbers in the epidermis and hair follicles [7]. These cells' ability to produce melanin and neural crest cell origin are their primary characteristics. People with more melanin typically have darker skin, eyes, and hair than those with less melanin [8]. In American Academy of Pediatrics Subcommittee on Hyperbilirubinemia studies in newborns tends to under-read in the lighter skin tone group while over-read in the darker skin tone group from the bilirubin test [9,10]. Van Erk *et al*., supported the finding with differences in tone group colour, including the characteristics of skin's light-scattering and the depth of the bone under the skin's surface, that can significantly impact bilirubin estimations in neonatal skin [11]. In the same vein, Kawano *et al.,* monitored skin colour changes in newborns to investigate neonatal jaundice non-invasively using image processing that shows detected bilirubin value towards full infants but not premature infants [12]. In surplus details, Karsten *et al.,* has modified the volume fraction of melanosomes in the epidermis, representing different skin types such as very fair, light, and dark, to allow the absorption test of models and use a simulation system as learning tool. It shows that learning is parallel based on the features of each skin colour.

From the light interaction through tissue perspective, less attention has been given on the effect of LED radial width distribution at different melanosome content and at varying bilirubin concentration. Besides that, different optode (emitter-detector) spacing can affect the light measured at the detector. This information can serve as valuable input when designing a real optical hardware for non-invasive jaundice detection. Given that, this project aims to investigate the effects of LED ray intensity distribution on three types of skin pigmentation (light skinned Caucasians, well-tanned Caucasians and Mediterranean, and dark skinned pigmented African) based on varying hyperbilirubinemia and excessive hyperbilirubinemia conditions using a simulation study approach. Following details are the simulation scopes of study:

i. forehead area was chosen as the site of tissue layers
ii. one million of photons at 470 nm (this wavelength corresponds better towards the detection of bilirubin [13]) was used to model light propagation in tissues

iii. LED radial width distribution at 30°, 40°and 60°
iv. average melanosomes concentration was applied on three skin types namely as light skinned Caucasians, well-tanned Caucasians and Mediterranean, and dark skinned pigmented African
v. bilirubin concentrations measured in mol/L for hyperbilirubinemia and excessive hyperbilirubinemia conditions
vi. optode spacing was set at 0.7 cm and 2 cm
vii. the simulation outcomes observed were based on diffuse reflectance and percentage of incident light collected on detector.

2. Methodology

Figure 1 represents a block diagram of the overall methodology:

i. Defining parameters
ii. Simulation in MCmatlab and lastly
iii. Performance evaluation.

First, the geometrical tissues layers, optical properties, melanosome volume fraction, bilirubin concentration, as well as LED radial width parameters were determined prior to conducting simulations in MCmatlab. The optimal wavelength for jaundice detection is at 470 nm (blue) because it is within the bilirubin's absorbance spectra, and therefore, corresponds to a better bilirubin detection [13]. The reflectance model design was employed with an emitter and detector placed adjacent to each other at 0.7 cm and 2 cm distance. A short source-detector separation (less than 20-25 mm) can be applied for non-invasive optical methods studies that are relatively superficial at most 1 cm deep. However, with long source-detector distances (greater than 40-50 mm), relatively less light is expected to reach the detector, and the signals might become noisy and unreliable [14]. Based on these facts, 0.7 cm and 2 cm were seemingly reasonable to be used in this study.

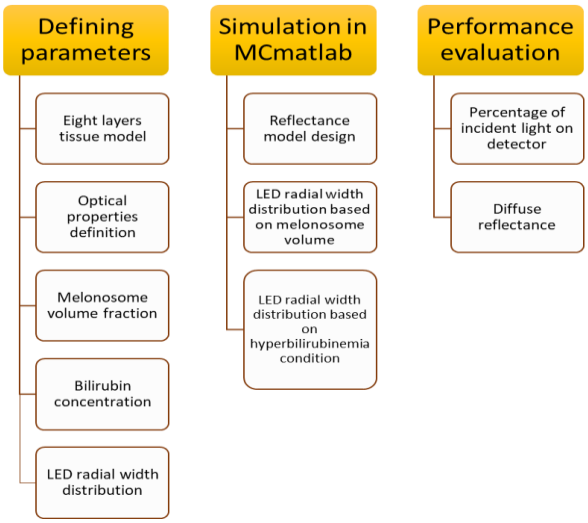

Fig. 1. The overall methodology of optical simulation in MCmatlab

2.1 Determination of Bilirubin and Melanosome Properties

Hyperbilirubinemia, more often known as jaundice, is a leading cause of a condition where blood bilirubin levels are exceeded in the body. Therefore, hyperbilirubinemia can be extremely harmful and potentially fatal for neonates. According to Iran J Public Health, during the first week of a newborn's life neonatal hyperbilirubinemia is a typical clinical issue in newborns who developed hyperbilirubinemia conditions, which are 8% to 11% [15]. Table 1 shows the range of hyperbilirubinemia and excessive hyperbilirubinemia.

Table 1
Range of hyperbilirubinemia and excessive hyperbilirubinemia for bilirubin concentration in g/L and mol/L [16]

Conditions	Bilirubin value (g/L)	Mol/L (for simulation study)
Hyperbilirubinemia	0.015	2.566×10^{-5}
	0.045	7.697×10^{-5}
	0.075	12.828×10^{-5}
Excessive hyperbilirubinemia	0.155	26.511×10^{-5}
	0.205	35.063×10^{-5}
	0.255	43.615×10^{-5}

A value less than 0.3 mg/dL (5.1 mol/L) of direct conjugated bilirubin is considered normal. However, the range of normal values for total bilirubin varies slightly between laboratories, ranging from 0.1 to 1.2 mg/dL (1.71 to 20.5 μmol/L). This paper considered two bilirubin conditions namely as hyperbilirubinemia and excessive hyperbilirubinemia with a set of spectra as 0.015, 0.045, and 0.075 g/L and 0.155, 0.205, and 0.255 g/L, respectively [16] to allow an estimation performance accuracy of serum levels of bilirubin.

Melanin is responsible for the coloration of body parts and guards against cell damage by absorbing UV (Ultraviolet) rays. A person's genes predetermine melanin levels; nevertheless, these levels are susceptible to change from various environmental factors, including age, sun exposure, and hormones [17]. Everyone has a varied skin colour, and there are significant variations even within the same race. Previous research by Jacques *et al.,* [18] has estimated melanosome volume fraction into three groups. This information can be applied to be tested on non-invasive jaundice applications. Table 2 shows three different skin pigmentations with average melanosome volume fraction. This data was used in the simulation.

Table 2
Average melanosomes per unit volume on each skin colour [18]

Skin colour	Average melanosomes volume fraction (%)
Light Skinned Caucasians	3.8
Well-Tanned Caucasians and Mediterranean	13.5
Dark Skinned Pigmented Africans	30.5

2.2 Determination of Geometrical Tissue Layer and Optical Properties

The optical properties of tissue layers, such as the thickness layers, scattering coefficient (μ_s), scattering anisotropy factor (g), and refractive index of tissue (n), can be found in Table 3. The specified thickness value is cumulative that increases gradually. The skin site of interest is centred on the newborn forehead region. The surface of the tissue was a homogeneous semi-infinite turbid medium as it helps to reduce the complexity in tissue modelling. Nine layers of geometrical layers

were specified in cuboid shape, and the size was 5 cm x 5 cm x 1.5 cm. There are distinct types of absorbers that can be found on each tissue layer.

Table 3
Tissue thickness and optical properties at 470 nm [19-21]

Air and Tissue Layers	Varying Tissue Thickness (mm)	Scattering Coefficient, μ_s (cm^{-1})	Anisotropy factor, g	Refractive index, n
Air	0.1	1×10^{-8}	1.0	1.0
Stratum corneum	0.01		0.7563	1.45
Living epidermis	0.08		0.76	1.4
Papillary dermis	0.1		0.76	1.4
Upper blood plexus	0.08		0.77	1.39
Reticular dermis	1.50	4.649×10^{3}	0.76	1.4
Deep blood plexus	0.07		0.7563	1.34
Dermis	0.16		0.76	1.4
Subcutaneous adipose tissue	4.0		0.7563	1.44

Table 4 shows the type of available absorber which is responsible for light absorption on skin. This information is important to be considered to ensure the multilayered tissue mimics skin absorption in light propagation. This light interaction of absorbed photons can provide a measure of when melanosome or bilirubin has a different value.

Table 4
The type of absorber found in each tissue layer

Skin layers	Absorber information
Stratum corneum	Melanosome
Living epidermis	Melanosome
Papillary dermis	Blood vessels, bilirubin
Upper blood plexus	Blood vessels, bilirubin
Reticular dermis	Blood vessels, bilirubin
Deep blood plexus	Blood vessels, bilirubin
Dermis	Blood vessels, bilirubin
Subcutaneous adipose tissue	Blood vessels, bilirubin

Multiple stackable tissue layers in MCmatlab were designed with tissue thickness according to the study parameters. An air layer was included as the top layer, followed by the eight-layered tissues consisting of stratum corneum, living epidermis, papillary dermis, upper blood plexus, reticular dermis, deep blood plexus, dermis, and subcutaneous adipose tissue layer. The detector and emitter were put side by side, with an applied intensity distribution, on top of the 3D model.

Eq. (1) was used to calculate the absorption coefficient by counting in the blood volume fraction, blood oxygen saturation, water, fat, melanosome volume fraction and bilirubin concentration content to mimic the skin properties absorption.

$$\mu_a = BS\mu_{a.oxy} + B(1-S)\mu_{a.deoxy} + W\mu_{a.water} + F\mu_{a.fat} + M\mu_{a.melanosome} + 2.3C_{bili \in bili} + 2.3C_{\beta C \in \beta C} \quad (1)$$

where,

B : average blood volume fraction ($f_{v.blood}$)
S : blood oxygen saturation (mm Hg)
W : water content volume fraction ($f_{v.water}$)
F : fat content volume fraction ($f_{v.fat}$)
M : melanosome volume fraction ($f_{v.melanosome}$)
Bili : bilirubin concentration (*C* (M))
βC : β-carotene concentration (*C* (M))

2.3 The Codebase of MCmatlab 3D Monte Carlo Simulations

The operating system in MCmatlab as an open-source codebase gives fast three-dimensional Monte-Carlo modelling of light transport in tissue and a MATLAB-based finite-element heat diffusion and Arrhenius-based thermal tissue damage simulator. Therefore, the codebase was modified to investigate the light distribution in a complex turbid environment, which is essential to simulate non-invasive jaundice study. Each tissue surface has a distinct type of boundary, and the flux is determined by the amount of reflection and transmission defined at the edge. The model simulation optical characteristics of tissues are utilized by the absorption (μ_a), scattering coefficient (μ_s), refractive index (n) and scattering anisotropy factor (g) which apply Beer's law to determine the appropriate numbers in all feasible scenarios [22]. The anisotropy factor (g) will help to measure the quantity of light dispersed in either a forward or backward direction after a scattering event. The scattering phase function will help define the new photon direction.

Figure 2 shows the entire steps in designing multilayer tissue in MCmatlab. A geometry definition model was considered by setting the number of bins and cuboid size. Next step, the optical properties as in Table 3 were assigned to the corresponding layers. Other pertinent parameters include setting the boundary type, emitter, and detector position as well as wavelength value. MCmatlab also provides a wide range of beam types namely pencil beam, isotropic emission point, an infinite plane wave, Laguerre-Gaussian LG01 beam, Radial-factorizable beam and X/Y factorizable beam.

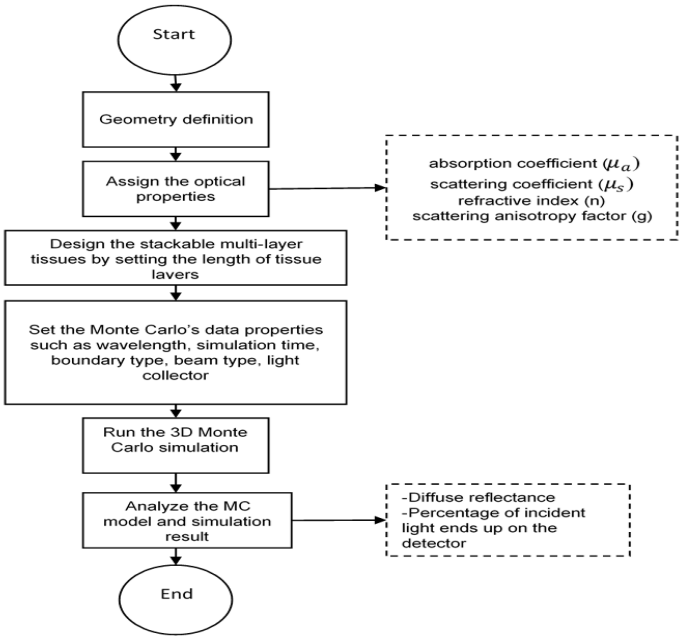

Fig. 2. The optical simulation steps in MCmatlab

Radial-factorizable beam was the emitter beam type employed in this study as it can be used to set the LED radial width distribution. For this study, three types of commercial blue LEDs with varied radial width distributions; 30°, 40°, and 60° were selected as indicated in Table 5. For Monte Carlo simulation, one million photons were injected into the tissue layers. The interactions of absorbed or scattered photons can provide a measure for light propagation resulting from changes in bilirubin and melanosomes in skin. Finally, the diffuse reflectance and percentage of incident light ends up on the detector were collected for analysis.

Table 5
Type of blue LEDs with different radial width distribution [23]

LED colour	Brand	Peak wavelength	Dominant wavelength	Radial width distribution
Blue	CreeLED 5-mm Blue Round LED [24]	480 nm	470nm	30° (pi/6)
	LED Blue Diffused 5mm Round T/H Würth Elektronik [25]	465 nm	470 nm	40° (2/9 pi)
	Blue LED Indication - Discrete 3.5V Radial [26]	-	470 nm	60° (pi/3)

2.4 Performance Evaluation

There were 108 simulation trials taken using two different optode spacing to evaluate the effect of radius width in the variation of bilirubin concentration and melanosomes in the optical simulation. Different bilirubin concentration values in this simulation were tested according to each melanosome average value, such as 3.8%, 13.5%, and 30.5%. Then, simulations were run accordingly for radius width with fixed values in bilirubin and melanosomes. As an evaluation of the data produced from MCmatlab, two main outcomes were focused on: diffuse reflectance and the percentage of incident light on the detector.

Diffuse reflectance is formed when the reflected from skin tissues scattered in all directions. Diffuse reflectance can be used as one of the simulation performances tools as it can reveal the differences on a molecular level between compared tissue settings. This is due to the fact that the skin has various layers that have certain refractive index values and layers such as the epidermis, dermis, and subcutaneous adipose tissue, where this model consists of a range of chromophores in 93-95% of the light that is scattered and absorbed [27,28]. Another simulation performance tool is the incident light absorbed by the detector. This is to see how much light has successfully reached the detector after varying optical properties, melanosome content, bilirubin concentrations and optode spacing.

3. Results and Discussion

3.1 The Geometrical Tissue Layers, Detectors and Emitters

The MCmatlab based on Monte Carlo simulation was successfully simulated for incident wavelength of 470 nm. Eight layers of skin tissue and an air layer were simulated with specified thicknesses as tabulated in Table 6.

Table 6
The thickness of multiple layers of tissue in bilirubin detection application

Number of layers	Cuboid layers	Thickness of tissue layers, d (cm)	In the MCMatlab (cm)
1	Air	0.1	0 – 0.1
2	Stratum corneum	0.001	0.1 – 0.101
3	Living epidermis	0.008	0.101 – 0.109
4	Papillary dermis	0.01	0.109 – 0.119
5	Upper blood plexus	0.008	0.119 – 0.127
6	Reticular dermis	0.15	0.127 – 0.277
7	Deep blood plexus	0.007	0.277 – 0.284
8	Dermis	0.016	0.284 – 0.3
9	Subcutaneous adipose tissue layer	0.4	0.3 – 0.7

Meanwhile, the resulting 3D tissue model can be viewed in Figure 3. Emitter and detector were presented visible on top of the model where it was placed next to each other with an optode spacing 0.7 cm. It should be noted that the distance was measured from centre to centre of emitter and detector, respectively. Then, optode separation at 2 cm was tested for comparison. The optical properties were applied to model the neonatal forehead tissues layer in Monte Carlo simulation. The amount of blood content (0.002), oxygen saturation (0.75), water (0.6) and fat (0.1) were applied into Eq. (1). These contents were defined as volume fractions, which is a one way of expressing a mixture's composition with a dimensionless unit. Hence, it would help to investigate how the LED radial width, melanosome, optode spacing behaves in the non-invasive jaundice application.

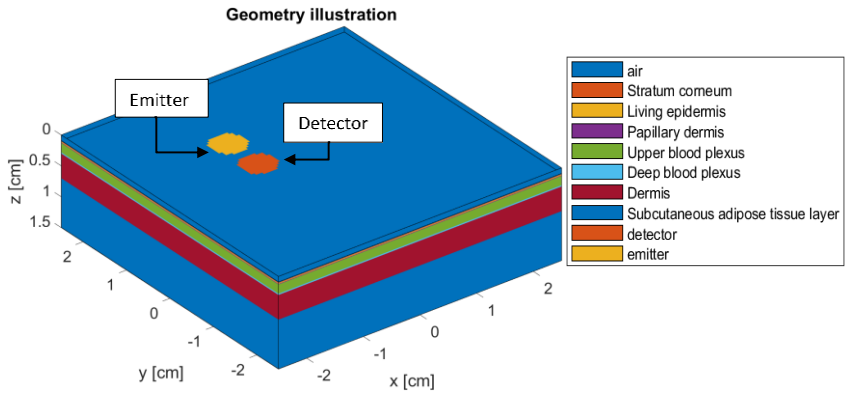

Fig. 3. An example of 3D geometry illustration of tissue design model

Figure 4 shows examples of the resulting photon pathways and normalized absorbed power per unit volume for optode distance at 0.7 cm. Figure 4(a) displays the photon pathway that successfully spread in the tissue model and the light reached about 0.7 cm in the depth of the subcutaneous adipose tissue layer. The 470 nm emitted light allows for the absorption, scattering and reflectance of light taken place through tissue layers. Meanwhile, Figure 4(b) shows the resulted normalized absorbed power per unit volume inside the tissue model for 60° of LED radial width. From the same figure, the red colour at the centre of cuboid denotes the highest absorbed power whereas the blue indicates the lowest absorbed power. One significant finding is the size area of the red colour will become bigger as the degree of LED radial width increased. From the simulations, it was found that the degree of LED radial width will affect the size of the area of normalized absorbed power. That is to say, the higher the degree of LED radial width, the bigger the size of normalized absorbed power area. On a different note, the optode distance does not have a significant impact on the absorbed power at the tissue. However, it plays a significant role when observing the incident light received by the detector.

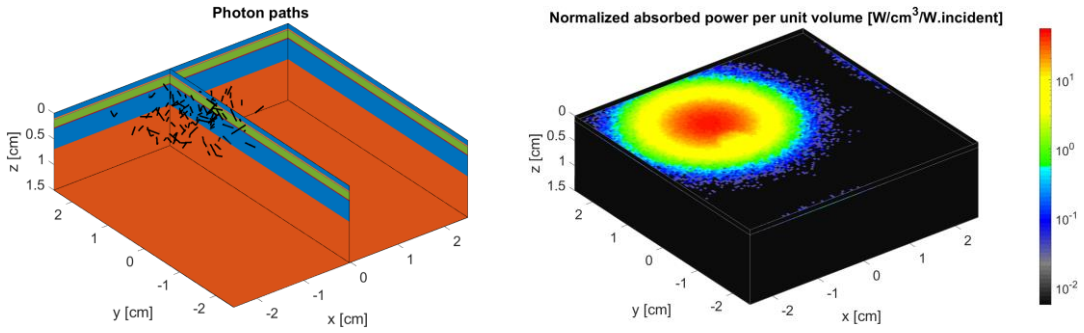

(a) (b)

Fig. 4. Examples of resulted optical simulation for 0.7cm at 60°: (a) Photon pathway and (b) Normalized absorbed power per unit volume absorbed by the cuboid

3.2 Number of Monte Carlo Simulation Trials

The simulations were performed in two different optode spacing that demonstrated the effect of LED radial width based on bilirubin and melanosome content. There was a total of 108 trials that were carried out in MCmatlab in which 54 trials were done for each optode spacing. Briefly, six bilirubin values as tabulated in Table 1 were simulated at 30°, 40° and 60° at three different types of skin at 0.7 cm optode spacing (6 bilirubin values x 3 LED radial width x 3 skin types=54 trials). Then, this process was repeated for 2 cm optode spacing. Average time taken to simulate each simulation was 5 minutes. For each trial, two outcomes will be recorded namely as diffuse reflectance and percentage of incident light ends up at detector.

3.3 Evaluation Performance of Diffuse Reflectance Based on LED Radial Width Variations

Figure 5(a), Figure 5(b), and Figure 5(c) show the data of 108 trials plotted as diffuse reflectance against bilirubin concentrations obtained from three skin types. From Figure 5(a), the LED radial width of 60° at optode spacing 2 cm (see left y-axis) resulted in a higher diffuse reflectance on all skin types (light, tanned, and dark) compared to the radial widths at 40° and 30°. With the use of optode spacing at 0.7 cm (see right y-axis), it displays smaller diffuse reflectance. This demonstrates how the optode spacing and LED radial width affects the outcome which shows the change in outcome value and how it is important in optical simulations in non-invasive jaundice detection for assuring that the observed light propagation on skin tissue layers can be appropriately assessed. The effect of melanosome was also found in non-invasive jaundice application where Figure 5(a) light skin colour have a higher diffuse reflectance compared to other hyperbilirubinemia skin colours conditions in Figure 5(b) tanned skin and Figure 5(c) dark skin colour. This is because lighter skin includes lesser melanosomes, which absorbs less light and has greater diffuse reflectance than tanned and dark skin, which have more melanosomes. This suggests that skin colour can influence diffuse reflectance which may help in diagnosis of bilirubin in non-invasive jaundice detection.

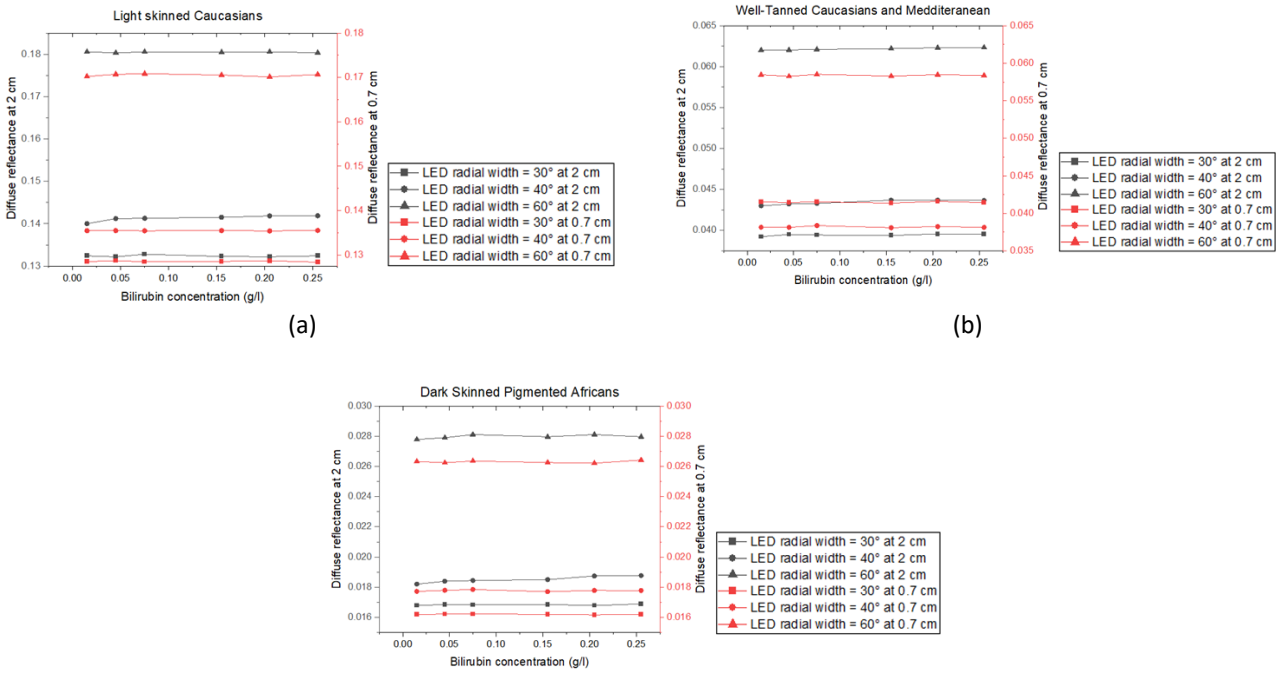

Fig. 5. Diffuse reflectance at 0.7 cm and 2 cm of optode spacing on a) Light Skinned Caucasians, b) Well-Tanned Caucasians and Mediterranean, and c) Dark Skinned Pigmented Africans in varied bilirubin concentration at 470 nm

3.4 Evaluation Performance of Percentage of Incident Light on Detector Based on LED Radial Width

Furthermore, the performance on percentage of incident light on detector is investigated by varying the parameters LED radial width, optode spacing, bilirubin and melanosome contents. Figure 6(a), Figure 6(b), and Figure 6(c) demonstrate the changes in percentage of incident light collected on the detector from the 108 trials in three different skin types using polynomial regression. At optode spacing 0.7 cm, the resulting incident light collected on detector is higher when the radial width is decreasing in emitting light on the tissue layer model. However, less incident light collected on detector at optode spacing 2 cm as the LED radial width decreases. Thus, it is more likely that the emitter-detector separation, radial width and scattering in the medium influenced the resulted outcome. On top of that, the percentage of light collected on light-skinned Caucasians (Figure 6(a)) resulting a higher percentage, followed by well-tanned skin (Figure 6(b)), and dark-skinned pigmented Africans colour (Figure 6(c)). The reason for the substantially different in simulation results of light collected on the detector in each type of skin with varied levels of bilirubin is most likely due to changes in melanosome content, as melanosome impact in light absorption and reflection on skin tissues [29]. Apart from that, the variable in bilirubin content, which may appear to be a contributing factor, impacts the light collected on the detector. Therefore, the results of this optical simulation study have shown that it is feasible to derive possible outcome values through simulation using commercially available surface-based Monte Carlo software and these parameters influence the light propagation in optical simulations can be used to expand the study of the effect of those variables in assessing the accuracy and optimal requirement in non-invasive jaundice detection.

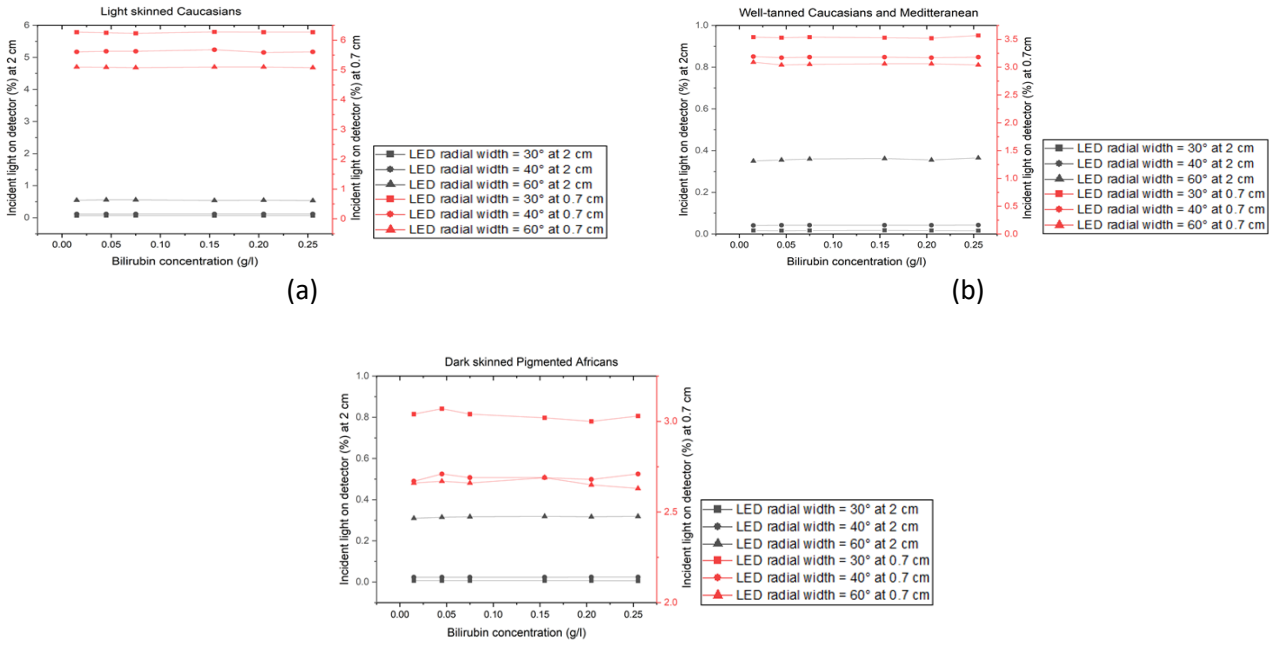

Fig. 6. Incident light absorbed by detector at 0.7 cm and 2 cm of optode spacing on: a) Light Skinned Caucasians, b) Well Tanned Caucasians and Mediterranean, and c) Dark Skinned Pigmented Africans at various bilirubin concentration

The findings above revealed that the incident light on the detector could help to analyse the percentage of light measured from the light skin interaction, whereas the diffuse reflectance light spread out helps to analyse the changes of reflected light, which contains results in bilirubin information under influenced of discussed factors. Therefore, both findings were significant in determining results in applying non-invasive jaundice since both display the changes in light intensity, contributed by factors as proposed in this project. According to the resulting incident light that ended up on the detector, the radial width of 30° at optode spacing 0.7 cm gives a better reading at the detector as it has a lower diffuse reflectance compared to 60°. At 60°, high diffuse reflectance was caused by high incoming parallel beams hitting different angles of tissue layers. Thus, it gives a lower reading of incident light on the detector. Therefore, the LED radial width of 60° is less suitable to be used on neonatal forehead skin tissue. Hence, a minimal radial width size should be considered.

4. Conclusions

In conclusion, all objectives set at the beginning of the research were successfully conducted. The stackable geometry tissue layers model in a cuboid shape with nine layers had been successfully defined by applying the optical properties, melanosome content, bilirubin concentrations, optode spacing and LED radial width distribution. The wavelength at 470 nm (blue) was approached as an optimal wavelength in this application. The effects of various LED radial width distributions based on optode spacing, melanosome and bilirubin content were simulated successfully using MCmatlab by analysing diffuse reflectance and the percentage of incident light absorbed by the detector. The use of LEDs considerably provides light reflection, allowing light reflectance to be viewed on the detector.

Overall, bilirubin, melanosome, spacing optode and LED radial width distributions greatly influenced the light propagation in the optical simulation of non-invasive jaundice application. The main results showed that the 30° LED radial width distribution resulted in distinct trends in 0.7 cm and 2 cm of optode spacing for all three types of skin. The amount of incident light collected on the

detector increased at LED radial width 0.7 cm, although diffuse reflectance decreased. However, diffuse reflectance and the proportion of incident light that was collected on the detector were both lower at an optode spacing 2 cm. In addition, because light skin colour absorbs less light and produces a higher reflection, these two measured results in diffuse reflectance on light skin increased by six times and the incident light collected on detector increased by one time greater than on tanned and dark skin.

In the future, the investigation of various optode spacings will be carried out to assure the optimal spacing in these simulation studies. Furthermore, the MCmatlab Monte Carlo simulation code may be modified to predict more practical and reliable findings based on the related parameters. As a result, the data gathered may be utilised to continue developing future optical hardware for the model to analyse bilirubin values non-invasively.

Acknowledgement
This research was supported by Universiti Tun Hussein Onn Malaysia (UTHM) through Tier 1 (vot Q545) and Ministry of Higher Education (MOHE) through Fundamental Research Grant Scheme (FRGS) (FRGS/1/2023/TK07/UTHM/02/13).

References

[1] Tousoulis, D., C. Antoniades, and C. Stefanadis. "Evaluating endothelial function in humans: a guide to invasive and non-invasive techniques." *Heart* 91, no. 4 (2005): 553-558. https://doi.org/10.1136/hrt.2003.032847
[2] Rizvi, Moattar Raza, Farah Mansoor Alaskar, Raid Saleem Albaradie, Noor Fatima Rizvi, and Khaled Al-Abdulwahab. "A novel non-invasive technique of measuring bilirubin levels using bilicapture." *Oman medical journal* 34, no. 1 (2019): 26. https://doi.org/10.5001/omj.2019.05
[3] Ngashangva, Lightson, Vinay Bachu, and Pranab Goswami. "Development of new methods for determination of bilirubin." *Journal of pharmaceutical and biomedical analysis* 162 (2019): 272-285. https://doi.org/10.1016/j.jpba.2018.09.034
[4] McEwen, Mark, and Karen Reynolds. "Noninvasive detection of bilirubin using pulsatile absorption." *Australasian Physical & Engineering Sciences in Medicine* 29, no. 1 (2006): 78-83.
[5] Lei, Mengjie, Tingting Liu, Yufeng Li, Yaqian Liu, Lina Meng, and Changde Jin. "Effects of massage on newborn infants with jaundice: A meta-analysis." *International journal of nursing sciences* 5, no. 1 (2018): 89-97. https://doi.org/10.1016/j.ijnss.2018.01.004
[6] Cheng, Nan-Yu, Yi-Ling Lin, Ming-Chien Fang, Wen-Hsien Lu, Chin-Chieh Yang, and Sheng-Hao Tseng. "Noninvasive transcutaneous bilirubin assessment of neonates with hyperbilirubinemia using a photon diffusion theory-based method." *Biomedical optics express* 10, no. 6 (2019): 2969-2984. https://doi.org/10.1364/BOE.10.002969
[7] Cichorek, Mirosława, Małgorzata Wachulska, Aneta Stasiewicz, and Agata Tymińska. "Skin melanocytes: biology and development." *Advances in Dermatology and Allergology/Postępy Dermatologii i Alergologii* 30, no. 1 (2013): 30-41. https://doi.org/10.5114/pdia.2013.33376
[8] Cleveland Clinic Medical, "Melanin." https://my.clevelandclinic.org/health/body/22615-melanin
[9] Wainer, Stephen, Yacov Rabi, Seema M. Parmar, Donna Allegro, and Martha Lyon. "Impact of skin tone on the performance of a transcutaneous jaundice meter." *Acta Paediatrica* 98, no. 12 (2009): 1909-1915. https://doi.org/10.1111/j.1651-2227.2009.01497.x
[10] American Academy of Pediatrics Subcommittee on Hyperbilirubinemia. "Management of hyperbilirubinemia in the newborn infant 35 or more weeks of gestation." *Pediatrics* 114, no. 1 (2004): 297-316. https://doi.org/10.1542/peds.114.1.297
[11] van Erk, Marlijn D., Alida J. Dam-Vervloet, Foky-Anna de Boer, Martijn F. Boomsma, Henrica van Straaten, and Nienke Bosschaart. "How skin anatomy influences transcutaneous bilirubin determinations: an in vitro evaluation." *Pediatric research* 86, no. 4 (2019): 471-477. https://doi.org/10.1038/s41390-019-0471-z
[12] Kawano, Sojiro, Thi Thi Zin, and Yuki Kodama. "A study on non-contact and non-invasive neonatal jaundice detection and bilirubin value prediction." In *2018 IEEE 7th Global Conference on Consumer Electronics (GCCE)*, pp. 401-402. IEEE, 2018. https://doi.org/10.1109/GCCE.2018.8574674
[13] Estepanian, Sevak. "Pulsating tissue simulator to study the detection of hyperbilirubinemia in neonates." PhD diss., California State University, Sacramento, 2018.

[14] Gratton, Gabriele, Carrie R. Brumback, Brian A. Gordon, Melanie A. Pearson, Kathy A. Low, and Monica Fabiani. "Effects of measurement method, wavelength, and source-detector distance on the fast optical signal." *Neuroimage* 32, no. 4 (2006): 1576-1590. https://doi.org/10.1016/j.neuroimage.2006.05.030
[15] Ullah, Sana, Khaista Rahman, and Mehdi Hedayati. "Hyperbilirubinemia in neonates: types, causes, clinical examinations, preventive measures and treatments: a narrative review article." *Iranian journal of public health* 45, no. 5 (2016): 558.
[16] Atencio, JA Delgado, S. L. Jacques, and S. Vázquezy Montiel. "Monte Carlo modeling of light propagation in neonatal skin." *Applications of Monte Carlo methods in biology, medicine and other fields of science* (2011): 297-314. https://doi.org/10.5772/15853
[17] D'Mello, Stacey AN, Graeme J. Finlay, Bruce C. Baguley, and Marjan E. Askarian-Amiri. "Signaling pathways in melanogenesis." *International journal of molecular sciences* 17, no. 7 (2016): 1144. https://doi.org/10.3390/ijms17071144
[18] Jacques, Steven L. "Optical absorption of melanin." *Oregon Medical Laser Center, http://omlc. ogi. edu/spectra/melanin/mua. html* (1998).
[19] Guedri, Kamel, Shougi Suliman Abosuliman, and Mowffaq Oreijah. "FTn Finite Volume Analysis of Ultrafast Laser Radiation Transport through Human Skin Cancer." *Applied Sciences* 10, no. 20 (2020): 7090. https://doi.org/10.3390/app10207090
[20] Lister, Tom, Philip A. Wright, and Paul H. Chappell. "Optical properties of human skin." *Journal of biomedical optics* 17, no. 9 (2012): 090901-090901. https://doi.org/10.1117/1.JBO.17.9.090901
[21] Katika, Kamal M., and Laurent Pilon. "Steady-state directional diffuse reflectance and fluorescence of human skin." *Applied optics* 45, no. 17 (2006): 4174-4183. https://doi.org/10.1364/AO.45.004174
[22] Shafie, Nur Fathin Amirah, Syazwani Mohd Faizo, Roshafima Rasit Ali, Mohd Yusof Hamzah, Naurah Mat Isa, Zatil Izzah Tarmizi, and Mohd Shahrul Nizam Salleh. "Laser Intensity of Thermo-Responsive Nanoparticles Size Measurement Using Dynamic Light Scattering." *Journal of Advanced Research in Fluid Mechanics and Thermal Sciences* 100, no. 2 (2022): 138-145. https://doi.org/10.37934/arfmts.100.2.138145
[23] "Data Sheet for 5mm Super Bright Blue LED 5A3 Series Class : Q Data Sheet For 5mm Super Bright Blue LED 5A3 Series Class : Q."
[24] Digi-Key Electronics. "CreeLED, Inc. C503B-BCN-CV0Z0462," https://www.digikey.com/en/products/detail/creeled-inc/C503B-BCN-CV0Z0462/2341542
[25] W. Elektronik, "151051BS04000 Datasheet WL-TMRC THT Mono-color Round Color," pp. 1–9.
[26] Digi-Key Electronics. "Lumex Opto/Components Inc. SSL-LX5093USBD," https://www.digikey.my/en/products/detail/lumex-opto-components-inc/SSL-LX5093USBD/468025
[27] Prince, Shanthi, and S. Malarvizhi. "Analysis of spectroscopic diffuse reflectance plots for different skin conditions." *Spectroscopy* 24, no. 5 (2010): 467-481. https://doi.org/10.1155/2010/791473
[28] Ash, Caerwyn, Michael Dubec, Kelvin Donne, and Tim Bashford. "Effect of wavelength and beam width on penetration in light-tissue interaction using computational methods." *Lasers in medical science* 32 (2017): 1909-1918. https://doi.org/10.1007/s10103-017-2317-4
[29] Markiewicz, Ewa, and Olusola Clement Idowu. "Melanogenic difference consideration in ethnic skin type: a balance approach between skin brightening applications and beneficial sun exposure." *Clinical, cosmetic and investigational dermatology* (2020): 215-232. https://doi.org/10.2147/CCID.S245043